APPENDIX A

Mohr's circle for two-dimensional stress

Compressive stresses have been taken as *positive* because we shall almost exclusively be dealing with them (as opposed to tensile stresses) and because this agrees with the universal practice in soil mechanics. Once this sign convention has been adopted we are left with no choice for the associated conventions for the signs of shear stresses and use of Mohr's circles.

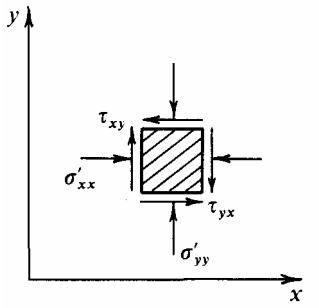

Fig. A.1 Stresses on Element of Soil

The positive directions of stresses should be considered in relation to the Cartesian reference axes in Fig. Al, in which it is seen that when *acting* on the pair of faces of an element *nearer* the origin they are in the *positive* direction of the parallel axis. The plane on which the stress acts is denoted by the first subscript, while the direction in which it acts is denoted by the second subscript. Normal stresses are often denoted by a single subscript, for example, σ'_x instead of σ'_{xx}.

For *Mohr's circle* of stress (Fig. A.2) we must take *counterclockwise* shear as *positive,* and use this convention *only* for the geometrical interpretation of the circle itself and revert to the mathematical convention for all equilibrium equations. Hence

X has coordinates $(\sigma'_{xx}, -\tau_{xy})$

and Y has coordinates $(\sigma'_{yy}, +\tau_{yx})$

But from equilibrium we require that $\tau_{xy} = \tau_{yx}$.

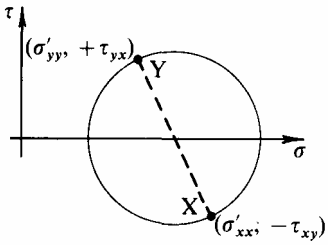

Fig. A.2 Mohr's Circle of Stress

Suppose we wish to relate this stress condition to another pair of Cartesian axes (*a*, *b*) in Fig. A.3 which are such that the counterclockwise angle between the *a*- and *x*-axes is $+\theta$.

Then we have to consider the equilibrium of wedge-shaped elements which have *mathematically* the stresses in the directions indicated.

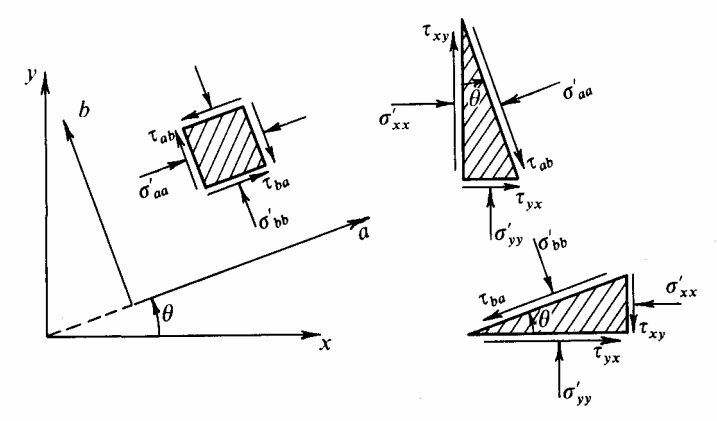

Fig. A.3 Stresses on Rotated Element of Soil

Resolving forces we get:

$$\left.\begin{aligned}
\sigma'_{aa} &= \frac{\sigma'_{xx}+\sigma'_{yy}}{2} + \frac{\sigma'_{xx}-\sigma'_{yy}}{2}\cos 2\theta + \tau_{xy}\sin 2\theta \\
\tau_{ab} &= \frac{-(\sigma'_{xx}-\sigma'_{yy})}{2}\sin 2\theta + \tau_{xy}\cos 2\theta \\
\sigma'_{bb} &= \frac{\sigma'_{xx}+\sigma'_{yy}}{2} - \frac{\sigma'_{xx}-\sigma'_{yy}}{2}\cos 2\theta - \tau_{xy}\sin 2\theta \\
\tau_{ba} &= -\frac{(\sigma'_{xx}-\sigma'_{yy})}{2}\sin 2\theta + \tau_{xy}\cos 2\theta = \tau_{ab}.
\end{aligned}\right\} \qquad \text{(A.1)}$$

In Mohr's circle of stress

A has coordinates $(\sigma'_{aa}, -\tau_{ab})$

and B has coordinates $(\sigma'_{bb}, +\tau_{ba})$.

A very powerful geometric tool for interpretation of Mohr's circle is the construction of the *pole,* point P in Fig. A.4. Through

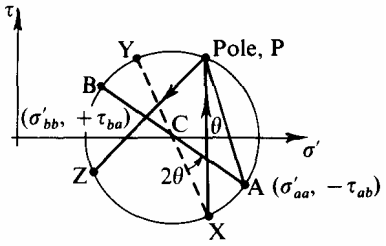

Fig. A.4 Definition of Pole for Mohr's Circle

any point on the circle a line is drawn parallel to the plane on which the corresponding stresses act, and the pole is the point where this line cuts the circle. In the diagram XP has been drawn parallel to the *y*-axis, i.e., the plane *on* which σ'_{xx} and τ_{xy} act.

This construction applies for *any* point on the circle giving the pole as a unique point. Having established the pole we can then reverse the process, and if we wish to know the stresses acting on some plane through the element of soil we merely draw a line through P parallel to the plane, such as PZ, and the point Z gives us the desired stresses at once.

This result holds because the angle XCA is $+2\theta$ (measured in the counterclockwise direction) as can be seen from eqs. (A.1) and by simple geometry the angle XPA is half this, i.e., $+\theta$ which is the angle between the two planes in question, Ox and Oa.

APPENDIX B

Typical input data of undrained triaxial test for processing by computer

DATA
PAL 556/OBSERVATIONS/2

T
T

TNORMALLY CONSOLIDATED SPESTONE III KAOLIN TO 60·8 P.S.I.
UNDRAINED TEST

TSTRAIN RATE ·0019 IN./MIN. DATE 6/8/65

1.25	Number of test
55·3155	Water content of initial slurry: (*a*) Wt of bottle and wet sample: gm
49·6691	(*b*) Wt of bottle and dry sample: gm
46·1257	(*c*) Wt of bottle: gm
3·851	Initial diameter of specimen: cm
3·848	
3·846	
3·853	
3·842	
3·848	
·01	Thickness of membrane: in
3·3626	Initial length of specimen: in
60·1067	Water content after preconsolidation. (Bottle weights as above)
51·2065	
38·2157	
14·62	Volume of water expelled during consolidation: cm^3
0	" " " " " test: cm^3
−8·265	" " " " " final unloading: cm^3
111·6228	Water contents of four samples from specimen at end of test after unloading (Bottle weights as above)
99·1068	
78·6222	
119·8637	
105·0578	
80·627	
118·4883	
104·2674	
81·0522	
119·423	
105·7703	
83·9292	Wt of final scraps of specimen on sheath, etc.
62·5111	
62·3748	
2·64	Specific gravity of soil particles
1720	Calibration factor of load measuring device: lb/in
·26	Value of λ
1·8	Zero value of pore-pressure transducer: lb/in^2
60·8	Maximum consolidation pressure: lb/in^2

0	Volume of water expelled during overconsolidation 'rebound' : cm^3
2·5	Membrane strength factor : lb/in
·05	Value of κ
3·46	$(\Delta V/V_0)/(\Delta l/l_0)$ during consolidation
60·8	Final pressure during consolidation : lb/in^2
1	Program instruction
81	Cell pressure during test : lb/in^2

1·474	500	21·8	First column — Vertical dial gauge readings : in
1·475	554	24·9	
1·476	577	26·5	Second column — Dial gauge readings of axial load measuring device : 10^{-4} in
1·477	591	27·1	
1·478	602	28·9	Third column — Pore-pressure readings : lb/in^2
1·479	611	30	
1·480	618	30·9	
1·481	624	32	
1·482	630	32·5	
1·484	640	33·6	
1·486	647	34·8	
1·488	654	35·6	
1·490	659·5	36·4	
1·492	665	37·2	
1·494	670	38	
1·496	675	38·9	
1·498	680	39·5	
1·500	685	40	
1·505	694	41·5	
1·510	702	43	
1·515	708·5	44·3	
1·520	714·5	45·1	
1·525	720	46·2	
1·531	725·7	47	
1·535	730	48	
1·540	733·8	48·5	
1·545	737·2	49·1	
1·550	740·5	49·8	
1·555	743·6	50·3	
1·560	746	51	
1·565	749	52	
1·570	751·2	52	
1·575	753·5	52·4	
1·580	755·5	53	
1·590	759	53·1	
1·600	762·2	54·5	
1·610	765	55	
1·621	768	55·6	
1·640	771	56·5	
1·660	777	57·1	
1·680	780·8	58	
1·700	784·8	58·5	
1·720	786·8	59·1	
1·740	788·1	59·8	
1·760	789	60·1	
1·777	791·5	60·5	
1·800	793	61	
1·821	794	61·2	
1·841	798·3	61·9	
1·860	799·3	62	
1·881	801	62·4	
1·900	803	62·4	
1·920	804·8	62·7	
1·940	806·5	63	
1·960	807	63	
1·980	807·8	63·1	
2·000	808	63·1	
2·020	808·1	63·1	
2·047	808	63·5	
2·051	806·6	63·5	
2·104	791·5	64	

Typical output data of undrained triaxial test processed by computer

JOB TITLE — (PAL 556/TRIAXIAL/1) . . . 23 5 66
STREAM NO. 1

NORMALLY CONSOLIDATED SPESTONE III KAOLIN TO 60·8 P.S.I. UNDRAINED TEST
STRAIN RATE ·0019 IN./MIN. DATE 6/8/65

TRIAXIAL TEST NO. 1.25

MC AFTER MIX			1·593	
INITIAL VOLUME CUB IN AND CC			5·902	96·722
MC AFTER TEST	TOP QUARTER		0·611	
	TOP HALF		0·606	
	BOTTOM HALF		0·613	
	BOTTOM QUARTER		0·625	
INITIAL MC AND VR		A	0·684	1·806
		B	0·695	1·834
		C	0·685	1·809

WHERE A FROM FINAL MC
B FROM INITIAL VOLUME
C FROM INITIAL MC

INITIAL VOLUME OF WATER CC 61·634
WEIGHT OF SOLIDS GRAM 90·108

AXIAL STRAIN	VOL STRAIN	SHEAR STRAIN	VOIDS RATIO	PORE PRESS	DEV STRESS	VP STRESS	Q P	Q PE	P PE
0·00000	0·00000	0·00000	1·377	0·00	0·00	61·00	0·000	0·000	1·000
0·00031	0·00000	0·00031	1·377	3·10	5·96	59·89	0·099	0·098	0·982
0·00062	0·00000	0·00062	1·377	4·70	8·49	59·13	0·144	0·139	0·969
0·00093	0·00000	0·00093	1·377	5·30	10·03	59·04	0·170	0·164	0·968
0·00124	0·00000	0·00124	1·377	7·10	11·24	57·65	0·195	0·184	0·945
0·00156	0·00000	0·00156	1·377	8·20	12·22	56·87	0·215	0·200	0·932
0·00187	0·00000	0·00187	1·377	9·10	12·99	56·23	0·231	0·213	0·922
0·00218	0·00000	0·00218	1·377	10·20	13·64	55·35	0·247	0·224	0·907
0·00249	0·00000	0·00249	1·377	10·70	14·30	55·07	0·260	0·234	0·903
0·00311	0·00000	0·00311	1·377	11·80	15·39	54·33	0·283	0·252	0·891

0·00374	0·00000	0·00374	1·377	13·00	16·14	53·38	0·302	0·265	0·875
0·00436	0·00000	0·00436	1·377	13·80	16·90	52·83	0·320	0·277	0·866
0·00499	0·00000	0·00499	1·377	14·60	17·49	52·23	0·335	0·287	0·856
0·00561	0·00000	0·00561	1·377	15·40	18·07	51·62	0·350	0·296	0·846
0·00624	0·00000	0·00624	1·377	16·20	18·61	51·00	0·365	0·305	0·836
0·00686	0·00000	0·00686	1·377	17·10	19·14	50·28	0·381	0·314	0·824
0·00749	0·00000	0·00749	1·377	17·70	19·67	49·86	0·395	0·322	0·817
0·00812	0·00000	0·00812	1·377	18·20	20·20	49·53	0·408	0·331	0·812
0·00968	0·00000	0·00968	1·377	19·70	21·14	48·35	0·437	0·347	0·793
0·01125	0·00000	0·01125	1·377	21·20	21·97	47·12	0·466	0·360	0·773
0·01283	0·00000	0·01283	1·377	22·50	22·63	46·04	0·492	0·371	0·755
0·01440	0·00000	0·01440	1·377	23·30	23·24	45·45	0·511	0·381	0·745
0·01598	0·00000	0·01598	1·377	24·40	23·79	44·53	0·534	0·390	0·730
0·01787	0·00000	0·01787	1·377	25·20	24·35	43·92	0·554	0·399	0·720
0·01914	0·00000	0·01914	1·377	26·20	24·78	43·06	0·575	0·406	0·706
0·02073	0·00000	0·02073	1·377	26·70	25·14	42·68	0·589	0·412	0·700
0·02231	0·00000	0·02231	1·377	27·30	25·45	42·18	0·603	0·417	0·692
0·02390	0·00000	0·02390	1·377	28·00	25·76	41·59	0·619	0·422	0·682
0·02550	0·00000	0·02550	1·377	28·50	26·04	41·18	0·632	0·427	0·675
0·02709	0·00000	0·02709	1·377	29·20	26·24	40·55	0·647	0·430	0·665
0·02869	0·00000	0·02869	1·377	30·20	26·51	39·64	0·669	0·435	0·650
0·03029	0·00000	0·03029	1·377	30·20	26·69	39·70	0·672	0·438	0·651
0·03189	0·00000	0·03189	1·377	30·60	26·89	39·36	0·683	0·441	0·645
0·03350	0·00000	0·03350	1·377	31·20	27·05	38·82	0·697	0·443	0·636
0·03671	0·00000	0·03671	1·377	31·30	27·31	38·80	0·704	0·448	0·636
0·03994	0·00000	0·03994	1·377	32·70	27·54	37·48	0·735	0·451	0·614
0·04317	0·00000	0·04317	1·377	33·20	27·72	37·04	0·748	0·454	0·607
0·04675	0·00000	0·04675	1·377	33·80	27·92	36·51	0·765	0·458	0·598
0·05294	0·00000	0·05294	1·377	34·70	28·02	35·64	0·786	0·459	0·584
0·05950	0·00000	0·05950	1·377	35·30	28·41	35·17	0·808	0·466	0·577
0·06610	0·00000	0·06610	1·377	36·20	28·57	34·32	0·832	0·468	0·563
0·07274	0·00000	0·07274	1·377	36·70	28·75	33·88	0·849	0·471	0·555
0·07943	0·00000	0·07943	1·377	37·30	28·72	33·27	0·863	0·471	0·545
0·08617	0·00000	0·08617	1·377	38·00	28·61	32·54	0·879	0·469	0·533
0·09295	0·00000	0·09295	1·377	38·30	28·47	32·19	0·884	0·467	0·528
0·09875	0·00000	0·09875	1·377	38·70	28·51	31·80	0·897	0·467	0·521
0·10665	0·00000	0·10665	1·377	39·20	28·39	31·26	0·908	0·465	0·512
0·11391	0·00000	0·11391	1·377	39·40	28·23	31·01	0·910	0·463	0·508
0·12089	0·00000	0·12089	1·377	40·10	28·41	30·37	0·936	0·466	0·498
0·12756	0·00000	0·12756	1·377	40·20	28·28	30·23	0·936	0·464	0·496

AXIAL STRAIN	VOL STRAIN	SHEAR STRAIN	VOIDS RATIO	PORE PRESS	DEV STRESS	VP STRESS	Q P	Q PE	P PE
0·13498	0·00000	0·13498	1·377	40·60	28·19	29·80	0·946	0·462	0·488
0·14174	0·00000	0·14174	1·377	40·60	28·15	29·78	0·945	0·461	0·488
0·14891	0·00000	0·14891	1·377	40·90	28·07	29·46	0·953	0·460	0·483
0·15613	0·00000	0·15613	1·377	41·20	27·99	29·13	0·961	0·459	0·478
0·16340	0·00000	0·16340	1·377	41·20	27·78	29·06	0·956	0·455	0·476
0·17073	0·00000	0·17073	1·377	41·30	27·61	28·90	0·955	0·453	0·474
0·17811	0·00000	0·17811	1·377	41·30	27·38	28·83	0·950	0·449	0·473
0·18555	0·00000	0·18555	1·377	41·30	27·14	28·75	0·944	0·445	0·471
0·19566	0·00000	0·19566	1·377	41·70	26·80	28·23	0·949	0·439	0·463
0·19718	0·00000	0·19718	1·377	41·70	26·63	28·18	0·945	0·436	0·462
0·21726	0·00000	0·21726	1·377	42·20	24·64	27·01	0·912	0·404	0·443

AXIAL STRAIN	VL	VK	DVK VDE	DQ PEDE	DP PEDE	Q PE	Q P	DVP DET
0·00016	3·444	2·583	−1·247	314·047	−58·738	0·049	0·050	1·247
0·00047	3·440	2·582	−0·858	133·513	−39·816	0·118	0·122	0·858
0·00078	3·438	2·581	−0·099	81·093	−4·579	0·152	0·157	0·099
0·00109	3·435	2·581	−1·618	63·596	−73·602	0·174	0·182	1·618
0·00140	3·430	2·580	−0·910	51·930	−40·606	0·192	0·205	0·910
0·00171	3·427	2·579	−0·770	40·282	−33·944	0·207	0·223	0·770
0·00202	3·423	2·579	−1·067	34·448	−46·397	0·218	0·239	1·067
0·00233	3·420	2·578	−0·345	34·415	−14·829	0·229	0·253	0·345
0·00280	3·418	2·578	−0·455	28·585	−19·393	0·243	0·271	0·455
0·00343	3·414	2·577	−0·593	19·861	−24·911	0·258	0·293	0·593
0·00405	3·410	2·576	−0·348	19·824	−14·400	0·271	0·311	0·348
0·00467	3·407	2·575	−0·387	15·462	−15·841	0·282	0·327	0·387
0·00530	3·404	2·575	−0·391	15·433	−15·837	0·291	0·342	0·391
0·00592	3·401	2·574	−0·408	13·966	−16·313	0·301	0·357	0·408
0·00655	3·398	2·574	−0·480	13·939	−18·928	0·309	0·373	0·480
0·00718	3·395	2·573	−0·284	13·912	−11·069	0·318	0·388	0·284
0·00780	3·393	2·573	−0·218	13·886	−8·452	0·327	0·401	0·218
0·00890	3·389	2·572	−0·325	9·844	−12·406	0·339	0·423	0·325
0·01047	3·382	2·571	−0·343	8·657	−12·777	0·353	0·452	0·343
0·01204	3·376	2·569	−0·310	6·910	−11·249	0·366	0·479	0·310
0·01361	3·371	2·569	−0·175	6·310	−6·224	0·376	0·501	0·175
0·01519	3·367	2·568	−0·272	5·714	−9·527	0·385	0·523	0·272
0·01693	3·363	2·567	−0·154	4·840	−5·304	0·395	0·544	0·154
0·01851	3·358	2·566	−0·328	5·515	−11·107	0·403	0·565	0·328
0·01993	3·355	2·565	−0·118	3·730	−3·928	0·409	0·582	0·118
0·02152	3·352	2·565	−0·154	3·265	−5·108	0·415	0·596	0·154
0·02311	3·349	2·564	−0·189	3·136	−6·172	0·420	0·611	0·189
0·02470	3·345	2·564	−0·130	2·898	−4·181	0·425	0·626	0·130
0·02629	3·342	2·563	−0·204	2·110	−6·491	0·429	0·640	0·204
0·02789	3·337	2·562	−0·299	2·759	−9·342	0·432	0·658	0·299

AXIAL STRAIN	VL	VK	DVK VDE	DQ PEDE	DP PEDE	Q PE	Q P	DVP DET
0·02949	3·334	2·561	0·020	1·866	0·622	0·436	0·671	−0·020
0·03109	3·333	2·561	−0·112	1·965	−3·436	0·439	0·678	0·112
0·03269	3·331	2·561	−0·183	1·627	−5·585	0·442	0·690	0·183
0·03510	3·329	2·560	−0·002	1·343	−0·062	0·446	0·700	0·002
0·03833	3·324	2·559	−0·226	1·165	−6·726	0·450	0·719	0·226
0·04156	3·318	2·558	−0·076	0·937	−2·220	0·453	0·742	0·076
0·04496	3·315	2·558	−0·086	0·885	−2·459	0·456	0·757	0·086
0·04984	3·310	2·557	−0·082	0·264	−2·295	0·458	0·775	0·082
0·05622	3·305	2·556	−0·042	0·991	−1·170	0·463	0·797	0·042
0·06280	3·300	2·555	−0·078	0·400	−2·102	0·467	0·820	0·078
0·06942	3·295	2·554	−0·041	0·436	−1·088	0·470	0·840	0·041
0·07609	3·291	2·553	−0·057	−0·079	−1·497	0·471	0·856	0·057
0·08280	3·286	2·552	−0·070	−0·257	−1·790	0·470	0·871	0·070
0·08956	3·281	2·551	−0·033	−0·356	−0·844	0·468	0·882	0·033
0·09585	3·278	2·551	−0·044	0·134	−1·085	0·467	0·890	0·044
0·10270	3·275	2·550	−0·046	−0·263	−1·126	0·466	0·902	0·046
0·11028	3·271	2·549	−0·023	−0·347	−0·567	0·464	0·909	0·023
0·11740	3·268	2·549	−0·063	0·423	−1·505	0·464	0·923	0·063
0·12422	3·264	2·548	−0·015	−0·329	−0·356	0·465	0·936	0·015
0·13127	3·262	2·548	−0·041	−0·203	−0·951	0·463	0·941	0·041
0·13836	3·260	2·547	−0·001	−0·099	−0·033	0·462	0·946	0·001
0·14533	3·258	2·547	−0·032	−0·170	−0·743	0·461	0·949	0·032
0·15252	3·256	2·546	−0·033	−0·195	−0·746	0·459	0·957	0·033
0·15977	3·254	2·546	−0·007	−0·452	−0·151	0·457	0·958	0·007
0·16707	3·253	2·546	−0·016	−0·387	−0·353	0·454	0·956	0·016
0·17442	3·252	2·546	−0·008	−0·509	−0·170	0·451	0·953	0·008
0·18183	3·251	2·545	−0·008	−0·525	−0·175	0·447	0·947	0·008
0·19061	3·248	2·545	−0·038	−0·555	−0·833	0·442	0·947	0·038
0·19642	3·246	2·544	−0·029	−0·908	−0·636	0·438	0·947	0·029
0·20722	3·240	2·543	−0·044	−1·624	−0·949	0·420	0·929	0·044

APPENDIX C

A yield function and plastic potential for soil under general principal stresses

The yield function, $F(p, q)$, for Granta-gravel, from eq. (5.27), is

$$F = q + Mp\left(\ln\frac{p}{p_u} - 1\right) = 0 \tag{C.1}$$

where

$$p = \frac{\sigma'_l + 2\sigma'_r}{3},\ q = \sigma'_l - \sigma'_r,\quad \text{and} \qquad p_u = \exp\left(\frac{\Gamma - v}{\lambda}\right).$$

We can treat the function F^* as a plastic potential in the manner of §2.10, provided we know what plastic strain-increments correspond to the stress parameters p and q. In §5.5 we found that $\dot{\upsilon}/\upsilon$ corresponded to p, and $\dot{\varepsilon}$ corresponded to q. Therefore, from eq. (2.13), we can first calculate

$$\frac{\partial F}{\partial q} = v\dot{\varepsilon} = 1,$$

so that the scalar factor v is

$$v = \frac{1}{\dot{\varepsilon}}, \tag{C.2}$$

and then we can calculate

$$\frac{\partial F}{\partial p} = v\frac{\dot{\upsilon}}{\upsilon} = \frac{1}{\dot{\varepsilon}}\frac{\dot{\upsilon}}{\upsilon} = M\ln\frac{p}{p_u} = \left(M - \frac{q}{p}\right).$$

This restates eq. (5.21) and thus provides a check of this type of calculation.

We wish to generalize the Granta-gravel model in terms of the three principal stresses and obtain a yield function $F^*(\sigma'_1, \sigma'_2, \sigma'_3, p_u)$ where p_u remains as specified above. Let us retain the same function as before, eq. (C.1), but introduce the generalized parameters of §8.2,

$$p^* = \left(\frac{\sigma'_1 + \sigma'_2 + \sigma'_3}{3}\right)$$

and

$$q^* = \frac{1}{\sqrt{2}}\left\{(\sigma'_2 - \sigma'_3)^2 + (\sigma'_3 - \sigma'_1)^2 + (\sigma'_1 - \sigma'_2)^2\right\}^{\frac{1}{2}}.$$

The function F^* then has equation

$$F^* = \frac{1}{\sqrt{2}}\left\{(\sigma'_2 - \sigma'_3)^2 + (\sigma'_3 - \sigma'_1)^2 + (\sigma'_1 - \sigma'_2)^2\right\}^{\frac{1}{2}} + M\left(\frac{\sigma'_1 + \sigma'_2 + \sigma'_3}{3}\right)\left\{\ln\left(\frac{\sigma'_1 + \sigma'_2 + \sigma'_3}{3p_u}\right) - 1\right\} = 0 \tag{C.3}$$

This function F^* generates a surface of revolution about the diagonal of principal stress space as shown in Fig. 5.1. Variation of p_u generates successive surfaces as indicated in Fig. 5.2.

Let us treat F^* as a plastic potential. Clearly, the stress parameters $(\sigma'_1, \sigma'_2, \sigma'_3)$ are associated with plastic strain-increments $(\dot{\varepsilon}_1, \dot{\varepsilon}_2, \dot{\varepsilon}_3)$ since the loading power is

$$\sigma'_1 \dot{\varepsilon}_1 + \sigma'_2 \dot{\varepsilon}_2 + \sigma'_3 \dot{\varepsilon}_3 = \frac{\dot{E}}{\upsilon}. \tag{C.4}$$

Therefore, from eq. (2.13) we calculate

$$\begin{aligned}
\frac{\partial F^*}{\partial \sigma'_1} &= v^* \dot{\varepsilon}_1 = \frac{3\{\sigma'_1 - [(\sigma'_1+\sigma'_2+\sigma'_3)/3]\}}{2\left\{\left[(\sigma'_2-\sigma'_3)^2 + (\sigma'_3-\sigma'_1)^2 + (\sigma'_1-\sigma'_2)^2\right]/2\right\}^{\frac{1}{2}}} + \frac{M}{3}\ln\left(\frac{\sigma'_1+\sigma'_2+\sigma'_3}{3p_u}\right) \\
\frac{\partial F^*}{\partial \sigma'_2} &= v^* \dot{\varepsilon}_2 = \frac{3\{\sigma'_2 - [(\sigma'_1+\sigma'_2+\sigma'_3)/3]\}}{2\left\{\left[(\sigma'_2-\sigma'_3)^2 + (\sigma'_3-\sigma'_1)^2 + (\sigma'_1-\sigma'_2)^2\right]/2\right\}^{\frac{1}{2}}} + \frac{M}{3}\ln\left(\frac{\sigma'_1+\sigma'_2+\sigma'_3}{3p_u}\right) \\
\frac{\partial F^*}{\partial \sigma'_3} &= v^* \dot{\varepsilon}_3 = \frac{3\{\sigma'_3 - [(\sigma'_1+\sigma'_2+\sigma'_3)/3]\}}{2\left\{\left[(\sigma'_2-\sigma'_3)^2 + (\sigma'_3-\sigma'_1)^2 + (\sigma'_1-\sigma'_2)^2\right]/2\right\}^{\frac{1}{2}}} + \frac{M}{3}\ln\left(\frac{\sigma'_1+\sigma'_2+\sigma'_3}{3p_u}\right)
\end{aligned} \tag{C.5}$$

If we introduce $\dot{\varepsilon}^*$, *a scalar* measure of distortion increment that generalizes eq. (5.6) and eq. (5.9), in the form

$$\dot{\varepsilon}^* = \frac{\sqrt{2}}{3}\left\{(\dot{\varepsilon}_2 - \dot{\varepsilon}_3)^2 + (\dot{\varepsilon}_3 - \dot{\varepsilon}_1)^2 + (\dot{\varepsilon}_1 - \dot{\varepsilon}_2)^2\right\}^{\frac{1}{2}} \tag{C.6}$$

then, as in eq. (C.3), we find from eq. (C.5) that

$$v^* = \frac{1}{\dot{\varepsilon}^*} \tag{C.7}$$

It is now convenient and simple to separate (C.5) into two parts:

$$\frac{\dot{\varepsilon}_1 + \dot{\varepsilon}_2 + \dot{\varepsilon}_3}{\dot{\varepsilon}^*} = M - \frac{q^*}{p^*}, \tag{C.8}$$

and

$$\begin{aligned}
\frac{\dot{\varepsilon}_2 - \dot{\varepsilon}_3}{\dot{\varepsilon}^*} &= \frac{3}{2}\frac{\sigma'_2 - \sigma'_3}{q^*} \\
\frac{\dot{\varepsilon}_3 - \dot{\varepsilon}_1}{\dot{\varepsilon}^*} &= \frac{3}{2}\frac{\sigma'_3 - \sigma'_1}{q^*} \\
\frac{\dot{\varepsilon}_1 - \dot{\varepsilon}_2}{\dot{\varepsilon}^*} &= \frac{3}{2}\frac{\sigma'_1 - \sigma'_2}{q^*}
\end{aligned} \tag{C.9}$$

The first part, eq. (C.8), is a scalar equation relating the first invariant of the plastic strain-increment tensor to other scalar invariants. The second part, eqs. (C.9), is a group of equations relating each component of a plastic strain-increment deviator tensor to a component of a stress deviator tensor. We will now show that these equations can be conveniently employed in two calculations.

First, we consider the corner of the yield surface. When $q^* = 0$ and $\sigma'_1 = \sigma'_2 = \sigma'_3 = p^*$, we find that eqs. (C.9) become indeterminate, but eq. (C.8) gives

$$\dot{\varepsilon}^* = \left(\frac{\dot{\varepsilon}_1 + \dot{\varepsilon}_2 + \dot{\varepsilon}_3}{M}\right) \tag{C.10}$$

Here, as in §6.6, we find that a plastic compression increment under isotropic stress is associated with a certain measure of distortion.

Next, we consider what will occur if we can make the generalized Granta-gravel sustain distortion in plane strain at the critical state where $(\dot{\varepsilon}_1 + \dot{\varepsilon}_2 + \dot{\varepsilon}_3) = 0.$ In plane strain $\dot{\varepsilon}_2 = 0,$ so at the critical state, $\dot{\varepsilon}_1 + \dot{\varepsilon}_3 = 0.$ With eqs. (C.9) these give

$$\frac{3}{2}\frac{\sigma'_2 - \sigma'_3}{q^*} = -\frac{\dot{\varepsilon}_3}{\dot{\varepsilon}^*} = +\frac{\dot{\varepsilon}_1}{\dot{\varepsilon}^*} = \frac{3}{2}\frac{\sigma'_1 - \sigma'_2}{q^*}$$

from which

$$\sigma'_2 = \frac{\sigma'_1 + \sigma'_3}{2}. \tag{C.11}$$

We satisfy this equation if we introduce the simple shear parameters (*s, t*) where $\sigma'_1 = s + t, \sigma'_2 = s, \sigma'_3 = s - t.$ In terms of these parameters, the values of p* and q* are

$$p^* = s \quad \text{and} \qquad q^* = \frac{1}{\sqrt{2}}\left\{t^2 + 4t^2 + t^2\right\}^{\frac{1}{2}} = \left(\sqrt{3}\right)t$$

The yield function *F** at the critical state reduces to

$$q^* - Mp^* = 0,$$

so that

$$t = \frac{M}{\sqrt{3}}s. \tag{C.12}$$

This result was also obtained by J. B. Burland[1] and compared with data of simple shear tests. In fact the shear tests terminated at the appropriate Mohr-Rankine limiting stress ratio before the critical state stress ratio of eqn. (C. 12) was reached.

[1] Burland, J. B. *Deformation of Soft Clay,* Ph.D. Thesis, Cambridge University, 1967.